

# MATRIX ANALYSIS OF AN FTPC LASER DISTRIBUTION MIRROR SYSTEM

James E. Draper  
University of California, Davis

April 1, 1999

## Abstract

Properties are derived for matrices needed to describe the trajectory of a laser beam through an arbitrary three-dimensional system of mirrors with arbitrary angles of orientation. From these ingredients, a computer program using Euler rotation matrices has been written which can be applied to the analysis of any mirror-only laser distribution system. The STAR TPC laser calibration system is an example of such a system. Using this program, an analysis is made of a hypothetical but reasonably realistic laser calibration system for the STAR FTPCs. The angular orientation of each mirror can be adjusted by a small rotation about either of two arbitrary but orthogonal axes in the plane of the mirror. The errors in beam positioning at each successive mirror are evaluated quantitatively, as produced by arbitrary adjustments of any subset of the mirrors. The ability to steer the beam reproducibly by remote control of the adjustments of two of the mirrors is considered. The stabilizing effect of having a tiny (1-mm) mirror just before the beam(s) through the FTPC gas is analysed. The effects of the mechanical shifting of the STAR magnet pole piece are shown to be unimportant.

## 1 INTRODUCTION

The main TPC of STAR has a laser calibration system<sup>[1]</sup> composed of a large number of 1-mm diameter laser beams at various locations and angular orientations throughout the sensitive volume of the TPC. Each of these beams produces a straight track of ionization in the TPC. These provide a means of mapping the possible distortions in the drift properties of the electron clouds from the tracks. The 1-mm beams are produced from a single, broad primary beam from a YAG laser, one at each end of STAR, from which are split these various beams by means of many 1-mm diameter mirrors. The centering of this broad beam is monitored by creating a Poisson spot at beam's center which is monitored by CCD cameras. A somewhat similar system of 1-mm mirrors is intended for the Forward TPCs (FTPCs), but not as extensive. About 15-18 beams per FTFC are expected.

It is important to assess the expected performance of this mirror system and to provide quantitative information about the extent of possible problems from tolerances and misalignments and about how to tune such a complex system. Each FTFC system is expected to have about 25 mirrors, and evidently they produce a cumulative effect on the beam. The purpose of the present analysis is to provide quantitative and representative results.

We consider a system of many mirrors, each with an arbitrary orientation in space. Each mirror is on a mount which permits control of the angular orientation of the mirror by adjustment of either or both of two screws on each mount. There is a three-point suspension on each mount, one point, W, being fixed while the locations of the other two points are adjusted by two screws, U and V. The distances UW and VW are of equal length and perpendicular to each other. The orientation of the mirror is controlled by adjustment of screws U and V. We will consider sending a laser beam through this system when the mirrors are calculated to be properly adjusted to provide the desired beam trajectory. This will provide the TUNED sets of points (x,y,z), each point being where the center of the beam strikes the surface of its mirror. Then we will twist some selected set of screws (i.e.,  $U_i$  and  $V_i$ ) on the mounts of the mirrors and find the resulting affect on the trajectory. Such affects will be given by listing the differences between the Cartesian coordinates of the new positions and those of the TUNED configuration.

## 2 REFLECTION MATRIX FOR MIRROR

Consider a mirror whose plane is parallel to the xy plane. The direction cosines of this mirror are (0,0,1). Denote the direction cosines of an arbitrary beam impinging on it as  $l_0, m_0, n_0$ . The action of the mirror on this beam is to

change the sign of  $n_0$  while having no effect on the beam's other two direction cosines. The matrix  $R_0$  accomplishes this as

$$R_0 \cdot \begin{pmatrix} l_0 \\ m_0 \\ n_0 \end{pmatrix} = \begin{pmatrix} l_0 \\ m_0 \\ -n_0 \end{pmatrix} \quad (1)$$

By inspection,

$$R_0 = \begin{pmatrix} 1 & 0 & 0 \\ 0 & 1 & 0 \\ 0 & 0 & -1 \end{pmatrix} \quad (2)$$

The next objective is to rotate this entire scenario, arbitrary beam impinging on and then reflecting from a mirror in the xy plane, by such an amount that the normal to the mirror is no longer parallel to the z axis, but has arbitrary direction cosines L, M, N. At this time we are not interested in the location of the mirror, only its orientation. Define such a rotation matrix P as

$$P = \begin{pmatrix} a & b & c \\ d & e & f \\ g & h & i \end{pmatrix} \quad (3)$$

The rotated scenario is

$$P \cdot R_0 \cdot \begin{pmatrix} l_0 \\ m_0 \\ n_0 \end{pmatrix} = P \cdot \begin{pmatrix} l_0 \\ m_0 \\ -n_0 \end{pmatrix} \quad (4)$$

or

$$[P \cdot R_0 \cdot P^T] \cdot [P \cdot \begin{pmatrix} l_0 \\ m_0 \\ n_0 \end{pmatrix}] = P \cdot \begin{pmatrix} l_0 \\ m_0 \\ -n_0 \end{pmatrix} \quad (5)$$

where  $P^T$  is the transpose of the matrix P. Being a rotation matrix, P is an orthogonal matrix so its rows are orthonormal, as are its columns. Also the inverse  $P^{-1} = P^T$ . The first square bracket is reflection matrix R for the arbitrarily oriented mirror, the second bracket is the incoming ray with the same angle of relative incidence as originally, and the right hand side is the resulting reflected ray.

Evaluating the first square bracket while making use of the orthonormality of the rows (or columns) gives

$$R = \begin{pmatrix} 1 - 2c^2 & -2cf & -2ci \\ -2cf & 1 - 2f^2 & -2fi \\ -2ci & -2fi & 1 - 2i^2 \end{pmatrix} \quad (6)$$

which is a symmetric matrix, unlike P. The new normal to the mirror is L, M, N, as defined above. So

$$P \cdot \begin{pmatrix} 0 \\ 0 \\ 1 \end{pmatrix} = \begin{pmatrix} c \\ f \\ i \end{pmatrix} \equiv \begin{pmatrix} L \\ M \\ N \end{pmatrix} \quad (7)$$

and the reflection matrix becomes

$$R = \begin{pmatrix} 1 - 2L^2 & -2LM & -2LN \\ -2LM & 1 - 2M^2 & -2MN \\ -2LN & -2MN & 1 - 2N^2 \end{pmatrix} \quad (8)$$

which is entirely determined by the direction cosines of the normal to the arbitrarily oriented mirror. Note that the sign of the vector normal to the mirror has no effect, as changing the signs of all of these direction cosines yields the same reflection matrix.

For illustration, consider that the incoming ray (second square bracket in Eq (5)) always has direction cosines 001 (traveling parallel to the z axis), and evaluate the reflected ray (right-hand side of Eq (5)) for various mirror orientations LMN. (Note that sometimes we omit the commas between direction cosines when the meaning is clear). For LMN = 001, the reflected ray, using Eq (8), is 00-1. For LMN=010, the reflected ray is 010, so this mirror has no effect. Similarly, for LMN=100 the reflected ray is 100 with no effect. For LMN=(1/√3, 1/√3, 1/√3) the reflected ray is (-2/3, -2/3, +1/3). As another illustration, consider an incoming ray of (1/√3, 1/√3, 1/√3) and a mirror of LMN=(1/√3, 1/√3, 1/√3). The reflected ray is (-1/√3, -1/√3, -1/√3). This ray is simply reversed in direction upon reflection.

### 3 EULER MATRIX TO ROTATE REFERENCE MIRROR TO ACTUAL ORIENTATION

We have in Eq (8) the reflection matrix for any arbitrary orientation of the plane of a mirror acting on any arbitrary incident ray and yielding its reflected ray. So far, the only used information about the mirror is the direction cosines of its normal. We also want to evaluate the effect of twisting screws U and/or V on the mirror mount. This means that we must know not only LMN, but also the orientation of an axis (UW or VW) in a plane parallel to the mirror surface. In order to incorporate this, we consider again a mirror whose plane is parallel to the xy plane. Consider that the axes WU and WV are parallel to the x and y axes in the laboratory. We denote this as the REFERENCE position of a mirror. We seek to determine the Euler rotation matrix (like P) which will rotate this mirror such that not only is the mirror's normal in the required TUNED direction LMN, but also the direction of mount-axis UW is the required TUNED one. That is, the mechanical mount of the mirror provides a particular direction LMN of the normal and a particular direction of axis WV (which determines WU for the TUNED configuration. After that, we want to evaluate the effect on the reflected ray resulting from a given twist of screws U and/or V away from the TUNED angular orientation of the mirror.

The procedure is as follows. We will find the direction of the normal to each mirror in the system in order to provide the required TUNED trajectory of the beam throughout the system of many variously oriented mirrors. Then for each mirror we will evaluate its Euler matrix to rotate that mirror mount from the standard REFERENCE orientation to this TUNED LMN orientation. This Euler matrix will also yield the final directions of axes UV and UW for its mount. Then we will hypothetically place this mirror back in its REFERENCE position and twist one or both of screws U and V by given amounts, evaluate the change in LMN of this mirror in the REFERENCE position, and finally use the same Euler matrix to determine the newly adjusted LMN of this mirror as a result of the adjustments of screws U and/or V. Note that the Euler matrix determines the orientation of the three axes of the mount, which before twisting screws U and/or V determines the mirror's LMN – after twisting, there is a slightly different LMN determined as just described.

The required matrix is P of Eq (3). Three of its elements are determined in Eq (7). The Euler matrix for rotation of a coordinate frame through the usual Euler angles  $\alpha$ ,  $\beta$  and  $\gamma$  is

$$Q^T(\alpha, \beta, \gamma) = \begin{pmatrix} \cos\beta \cdot \cos\alpha \cdot \cos\gamma & \cos\beta \cdot \sin\alpha \cdot \cos\gamma & -\sin\beta \cdot \cos\gamma \\ -\sin\alpha \cdot \sin\gamma & +\cos\alpha \cdot \sin\gamma & \\ -\cos\beta \cdot \cos\alpha \cdot \sin\gamma & -\cos\beta \cdot \sin\alpha \cdot \sin\gamma & \sin\beta \cdot \sin\gamma \\ -\sin\alpha \cdot \cos\gamma & +\cos\alpha \cdot \cos\gamma & \\ \sin\beta \cdot \cos\alpha & \sin\beta \cdot \sin\alpha & \cos\beta \end{pmatrix} \quad (9)$$

The definition of these Euler angles <sup>[2]</sup> is that in sequence, the coordinate frame is: (a) rotated about the old z axis through the angle  $\alpha$ ; (b) rotated about the new y axis through the angle  $\beta$ ; (c) rotated about the new z axis by the angle  $\gamma$ . The transpose of this is the Euler matrix for rotating a vector. The latter matrix is what we use here, so we named Eq (9) as the transpose. From Eq (7), the terms in the bottom row of Eq (9) are L, M, N, respectively, so we have a means to evaluate some properties of  $\alpha$  and  $\beta$ . In other words, the first two rotations in the above sequence are the ones that determine the direction, apart from the sign, of the normal to the actual mirror. The final rotation through angle  $\gamma$  determines the orientation of axes UV and UW. Of course, knowing the direction LMN and the direction of either of axes UW or VW provides the other axis because the system is right handed. From this sequence of three rotations we see that the polar coordinates  $\theta$  and  $\phi$  of the old z axis, or normal to mirror, after the first two (or all three) Euler rotations are  $\phi = \alpha$  and  $\theta = \beta$ .

Thus, the relation of the first two Euler angles to the mirror normal is

$$\begin{aligned} \cos\beta &= N \\ \cos\alpha &= L/\sqrt{1-N^2} \end{aligned} \quad (10)$$

Only L and N are needed in Eq (10), but they are not enough to determine the normal completely. Although (L, M, N) is normalized, the sign of M is still undetermined. That sign is determined from the requirement that the columns of the Euler matrix are orthonormal to each other, as are the rows. Knowledge of L and N restricts the normal vector to be on the intersection of a cone around the x axis and a cone around the z axis. However, there are two such lines of intersection, so the value of M is also needed to determine the orientation of the normal. On the other hand, knowledge of only  $\alpha$  and  $\beta$  is enough to uniquely determine the direction of the normal. This apparent contradiction is resolved by noting the Eq (10) leaves  $\alpha$  and  $\beta$  each uncertain as to algebraic sign.

We know that the bottom row of Eq (9) is L M N. We can use either of the upper two elements of the third column of Eq (9) to get information about the third Euler angle, hence the remainder of the Euler matrix. For example,

$$\sin\gamma = h/\sqrt{(1 - N^2)}. \quad (11)$$

Here it is unclear whether we have evaluated  $\gamma$  or  $\pi - \gamma$ , as in the discussion above. By evaluating the result of the Euler matrix Q (transpose of Eq (9)) acting on a unit vector along x, y or z, we see that the first column of Q (first row in Eq (9)) is the direction cosines of the "x" axis of the mirror mount, denoted Xside. The second column of Q (second row in Eq (9)) is the direction cosines of the "y" axis of the mirror mount, denoted Yside. The third column of Q has already been recognized as the direction cosines of the normal to the mirror. Here "x" and "y" refer to the x and y axes in the REFERENCE position. They will have new directions after application of the Euler matrix, and these directions must match the actual mechanical design of the placement of the mirror mount. Conversely, calculations that are made possible with the present discussion can help to determine what the orientation of the Xside and Yside should be.

The ambiguities in the Euler angles, just discussed, can sometimes be resolved by the straightforward use of Eqs (10) and (11), followed by a simple test. That is, one can fabricate a simple, rotatable coordinate system by straightening three paper clips, bending each into an "L" shape and taping these three together to form an orthogonal coordinate system. Label the axes with tape to form a right-handed system. Then manipulate this triad by hand through the prescribed three rotations of the Euler matrix and it can be determined which solution of Eqs (10) and (11) is appropriate.

This can also be checked by recalling that these matrix elements are the cosines of the angles between the laboratory x, y or z axes and the actual normal and the adjustment axes (WU and WV) produced by the Euler rotation matrix Q operating on the x, y and z unit vectors, using these values of  $\alpha$ ,  $\beta$  and  $\gamma$ . For example, suppose that we want the adjustment axis WU to be horizontal for the TUNED mount. This means  $d=0$  in Eq (3), so  $Q_{21}=0$ , so  $\tan\gamma=-MN/L$ . This gamma, determined from L, M and N, will yield a horizontal WU axis in the actual mirror mount. However, there is still the question of the signs of the three Euler angles determined from these relations.

Conversely, having determined  $\alpha$ ,  $\beta$  and  $\gamma$ , the Euler matrix is uniquely determined from Eq (9). Now we have an Euler matrix for each mirror which properly orients its TUNED mount, including providing the correct orientations of the normal and adjustment axis WU. The reflected ray from any of these mirrors for a given incident ray is now determined by its TUNED LMN.

## 4 MATRIX FOR DRIFT BETWEEN MIRRORS

The drift of the beam between a pair of mirrors involves the distance D between the point  $(x_i, y_i, z_i)$  where the beam leaves the surface of the upstream mirror and the point  $(x_f, y_f, z_f)$  where the beam strikes the surface of the succeeding mirror. The beam has direction cosines (l,m,n) between these two mirrors. The relation is

$$\begin{pmatrix} x_f \\ y_f \\ z_f \\ 1 \end{pmatrix} = \begin{pmatrix} 1 & 0 & 0 & lD \\ 0 & 1 & 0 & mD \\ 0 & 0 & 1 & nD \\ 0 & 0 & 0 & 1 \end{pmatrix} \cdot \begin{pmatrix} x_i \\ y_i \\ z_i \\ 1 \end{pmatrix} \quad (12)$$

as can be seen by evaluating the right-hand side of Eq (12). This drift matrix in Eq (12) will be denoted as S.

For different values of (l,m,n), the beam starting at the point  $(x_i, y_i, z_i)$  will not travel exactly the same distance before striking the next mirror. We want to accurately evaluate D, defined as positive. The equation for a plane at a distance p, defined as positive, from the origin is

$$Lx + My + Nz = p, \quad (13)$$

where the direction cosines of the normal to the plane are L, M, N, while (x,y,z) is any point in the plane. If we require this point to be  $(x_f, y_f, z_f)$ , then using the values of  $(x_i, y_i, z_i)$  from Eq (12), we find

$$D = [p - Lx_i - My_i - Nz_i]/[Ll + Mm + Nn]. \quad (14)$$

Next we employ another application of Eq (13) for the same plane where the point in the plane is  $(x_c, y_c, z_c)$ , being ideally defined as fixed regardless of the twisting of the two adjustment screws. Such a point, for example, would be the center of the mirror surface for a gimbal mount, discussed below. This can be used to eliminate p, and give

$$D = [L(x_c - x_i) + M(y_c - y_i) + N(z_c - z_i)]/[Ll + Mm + Nn] \quad (15)$$

Incidentally, the denominator is the cosine of the angle between the directions l,m,n and L,M,N, which observation will help in verifying Eq (15) by trigonometry.

If the mount and mirror had zero thickness between point W (pivot point for adjustments U and V, discussed above) and the mirror surface, then point W would have the coordinates  $(x_c, y_c, z_c)$ . A better approximation, more accurate and easier to apply, is that the point  $(x_c, y_c, z_c)$  is the point where the TUNED beam strikes this mirror. For either approximation the effect on the accuracy of the trajectory is negligible for the dimensions of the system at STAR.

## 5 EFFECT ON MIRROR NORMAL FROM ADJUSTING SCREW

Twisting the adjustment screw U yields a rotation of the normal to the mirror about the axis WV. Similarly, adjusting screw V yields a rotation of the normal to the mirror about axis WU. The easiest way to determine the affect of such adjustment on the subsequent trajectory is to adjust it in the REFERENCE position, and to transform the result with the same Euler matrix. That is, the base of the mount is the same before and after the screw adjustment, and the Euler matrix positions the base.

Another rotation matrix describes each of the adjustments of screws U and V. We know that mechanically a three-point suspension determines the plane of the mirror, and the order of adjustment of screws U and V should not matter. On the other hand, rotation matrices do not commute, in general. However, it is easy to prove that when the sines of the two angles of rotation are  $\ll 1$ , the two rotation matrices commute. Then the combined effect of the two rotations is the transformation matrix

$$\begin{pmatrix} 1 & 0 & -\sin\epsilon \\ 0 & 1 & \sin\delta \\ \sin\epsilon & -\sin\delta & 1 \end{pmatrix} \quad (16)$$

where  $\delta$  is the angle through which the mirror's normal would rotate when only the screw which rotates about the x axis (REFERENCE orientation) is twisted. Similarly  $\epsilon$  is the angle through which the mirror's normal would rotate when only the screw which rotates about the y axis is twisted. We will see that  $\delta$  and  $\epsilon$  of only a few milliradians can produce intolerably large deviations of the trajectory from the TUNED trajectory, so the approximation represented by Eq (16) is good for relevant adjustments.

Now the adjusted normal in the REFERENCE orientation is the product of the matrix in Eq (16) operating on the normal,  $(0,0,1)$ , which yields  $(-\sin\epsilon, +\sin\delta, 1-\sin^2\delta - \sin^2\epsilon)$ . When this result is operated on by the Euler matrix Q obtained from Eq (9) for the TUNED configuration, the ADJUSTED TUNED normal is obtained. These new adjusted values of the direction cosines of the mirror normal for any mounts that have been adjusted away from the TUNED configuration are used in determining the trajectory after screw adjustment of the mirror system.

## 6 KINEMATIC MOUNTS AND GIMBAL MOUNTS OF MIRRORS

The meaning of the term "kinematic mount" is illustrated by the last paragraph of section 1. Here the fixed point is the central point W between the points of contact of the two adjusting screws, U and V. This results in a slightly altered distance D of drift to a mirror that has been adjusted, as discussed near Eq (15).

The "gimbal mount" is one designed such that the center of the mirror on this mount is the point that does not change coordinates when its adjusting screws are twisted. This is more complicated to construct.

It is already noted above that there is no practical difference in the accuracy of the calculations for the systems discussed here when either type of mount is used. For either type of mount, the point  $(x_c, y_c, z_c)$  will here be defined as the point where the beam strikes this mirror for the TUNED configuration.

The adjusting screws are often 80 threads per inch. Kinetic mount manufacturers say that a sensitive hand can detect  $1^\circ$  of twist of the screw. This would indeed seem to be the limit of sensitivity! If the distances UW and VW are 10 mm, approximately true in minimounts, this  $1^\circ$  twist corresponds to 0.09 milliradian. Since a  $10^\circ$  twist is only 1.7 minutes movement of the minute hand of a clock, we will use 1 milliradian as a typical and somewhat reproducible adjustment for the present calculations.

## 7 TEST CALCULATIONS

A computer program has been written using the relations above. These tests will be described in some detail in order to illustrate features and problems of dealing with these variables. The inputs to the program for each leg

Table 1: Euler matrices for the TUNED positions of Case A.

<i>Mirror1</i>			<i>Mirror2</i>			<i>Mirror3</i>		
$1/\sqrt{2}$	0.00	$-1/\sqrt{2}$	$1/\sqrt{2}$	0.00	$1/\sqrt{2}$	$-1/\sqrt{2}$	0.00	$1/\sqrt{2}$
0.00	1.00	0.00	0.00	1.00	0.00	0.00	1.00	0.00
$1/\sqrt{2}$	0.00	$1/\sqrt{2}$	$-1/\sqrt{2}$	0.00	$1/\sqrt{2}$	$-1/\sqrt{2}$	0.00	$-1/\sqrt{2}$

Table 2: Angles  $\delta$  and  $\epsilon$  (milliradians) resulting from twisting the screws on each mirror mount, and the resulting errors (mm) in position of striking the succeeding mirror (or after 1000 mm of travel for the last leg).

<i>mirror</i>	$\delta$	$\epsilon$	$err_x$	$err_y$	$err_z$
1	0.0	1.0	1.9999	0.0000	1.9958
2	0.0	1.0	1.9999	0.0000	-2.0039
3	0.0	1.0	1.9980	0.0000	-4.0038
1	1.0	0.0	-0.0009	1.4142	0.0010
2	1.0	0.0	-0.0029	4.2427	-0.0031
3	1.0	0.0	-0.0118	8.4853	-0.0061
1	1.0	1.0	1.9990	1.4100	1.9970
2	1.0	1.0	1.9969	4.2497	-2.0068
3	1.0	1.0	1.9859	8.4909	-4.0098

of the laser beam are the distance to the center of the next mirror in the TUNED position and the three Euler angles of the TUNED mirror. Also input are the coordinates of the starting point of the beam and the direction cosines of this initial beam. Checks are made in the program to determine that each Euler matrix generated has orthonormal rows and orthonormal columns and that the each Euler matrix transforms unit vectors along the axes in the REFERENCE system to form a right-handed system. We will illustrate applications of this program by two test cases and by an example of a realistic geometry for the FTPC laser system.

Case A is defined as a 1000 mm square array of legs of laser beam travel. That is, the beam starts at the origin, travels 1000 mm in the positive z direction to the first mirror which reflects the beam at right angles so it travels along the negative x direction. This beams travels to a second mirror, followed by a right-angle reflection, followed by a third mirror and its right-angle reflection. All of the trajectory is intended to be in a plane. This third reflected beam is allowed to travel a fixed distance of 1000 mm. Thus, each leg is 1000 mm long in the TUNED condition. For this case, the accuracy of the computations is checked by noting how far from the origin is the fourth leg of the trajectory after 1000 mm of travel – this distance should be vanishingly small.

To illustrate quantitatively, the direction cosines of the successive beams in the four legs in the TUNED location are (0,0,1), (-1,0,0), (0,0,-1) and (1,0,0). There is a mirror after each of the first three of these beams. The direction cosines of the normals to the mirrors are  $(1/\sqrt{2},0,1/\sqrt{2})$ ,  $(-1/\sqrt{2},0,1/\sqrt{2})$  and  $(-1/\sqrt{2},0,-1/\sqrt{2})$ . The distance between the origin of the first beam and the computed arrival point of the fourth beam is 0.0004 mm after a path length of 4000 mm. A computer precision carrying seven digits was used for all the computations presented here. The Euler matrices, whose transpose is shown in Eq (9), are listed in Table 1. The numerical results differed from these values by  $\leq \pm 2$  in the seventh digit. The matrices of Table 1 are used to rotate the normal to each of the mirror mounts from the REFERENCE position around to the TUNED orientation. The Euler angles (degrees) that produced Table 1 are  $(\alpha, \beta, \gamma)=(0, 45, 0)$ ,  $(0, -45,0)$  and  $(0,-135,0)$ , respectively. Note that the bottom row in each matrix is the same as the direction cosines of the normal to the mirror, described above. Similarly the middle row is the direction cosines of the Yside of the mirror mount. All Ysides are parallel. And the top row is the Xside of each mirror, each Xside being 90° clockwise beyond its predecessor (looking down on the upward pointing y axis of the coordinate system).

Next are the deviations from this TUNED situation when screw adjustments are made. Table 2 shows the adjustment angles,  $\delta$  and  $\epsilon$ , from the TUNED position of each mirror and the accompanying difference between the resulting locations where the beam strikes the mirror compared to the locations of the points where the beams strike the mirrors in the TUNED positions. The angles  $\delta$  and  $\epsilon$  represent the movement of the normal to the mirror in the REFERENCE position resulting from twisting the adjusting screws in the kinetic mounts. Angle  $\delta$  is an adjustment about the axis Xside;  $\epsilon$  is and adjustment about the axis Yside. We see that the errors are roughly additive, in the sense that the errors in the bottom group,  $\delta=1.0$ ,  $\epsilon=1.0$ , are nearly the sum of those of the first two groups. This is related to the fact that the angles  $\delta$  and  $\epsilon$  in the bottom group are the sums of those in the first two groups.

Case B: In order to try a case where we know the answers to expect, but have a more complex three-dimensional

Table 3: Euler matrices for Case B.

<i>Mirror1</i>		
-0.4571067	0.2499999	-0.8535534
-0.8535534	0.1464467	0.5000000
0.2500000	0.9571068	0.1464465
<i>Mirror2</i>		
-0.2500004	-0.9571068	-0.1464458
-0.8535532	0.1464474	0.5000000
-0.4571068	0.2499999	-0.8535535
<i>Mirror3</i>		
-0.4571067	0.2499999	-0.8535534
-0.8535534	0.1464467	0.5000000
0.2500000	0.9571068	0.1464465

problem to calculate and to visualize, we rotate the entire system of Case A using an Euler matrix composed of  $45^\circ$  angles for each of  $\alpha$ ,  $\beta$  and  $\gamma$ . We make an Euler transformation of every leg of beam travel, the normal to every mirror and the Yside and the Xside of every mirror in order to see what the computed results should look like. In other words, we tip the square three dimensionally without distorting it. However, as usual, we only input the initial beam, the three Euler angles of each mirror transformation from the REFERENCE position to the TUNED position, and the distance between each successive pair of mirrors measured center to center in the TUNED position. But how should we find the Euler angles needed to match a chosen mechanical design of the laser system? They are not obvious for a complicated system of mirrors where we start with only the desired trajectory of the laser beam as it travels from the laser to the entirety of the system.

The method used to determine the Euler angles for each mirror is as follows: Recall that the three Euler angles completely determine the nine elements of the Euler matrix. First, select the desired normal to the mirror and select the (2,3) element of the Euler matrix. The direction cosines of the desired normal determine the bottom row of the Euler matrix. Its (2,3) element fixes the z (lab frame) component of the Yside of the mirror mount. This does not completely determine the Euler matrix since the direction of the Yside is not fully determined – it has two possible values. Rather than develop further algebra for this problem, a program was written to use these four input numbers ((3,1), (3,2) (3,3) and (2,3) elements of the Euler matrix) to find a solution for the Euler angles, as in Eqs (10-11). Then all eight combinations of signs of these three Euler angles are tried and the Euler matrix for each combination is calculated. By comparing the rows of each of these eight matrices to the desired geometry of the mirror mount we find that at most only one of the eight solutions is satisfactory.

For example, for Case B we want the Ysides of all three mirrors to be parallel to each other, as they were in Case A. Sometimes the above eight solutions will contain only one possible candidate but that candidate has a flaw – viz., the Yside has the correct direction and the normal has the correct direction apart from the sign. This means that the normal’s direction is opposite to the direction of the normal in Case A after transformation by the above three  $45^\circ$  Euler angles. As the sign of the normal does not matter for the reflection from the mirror, this candidate solution would be satisfactory except that the Xside is pointing  $180^\circ$  away from its desired position. This is because the normal is reversed and the systems are always right handed. This means that  $\delta$  would produce the wrong sign of effect. So for the two mirrors for which this happened, the opposite sign of  $\delta$  was selected for Table 4 compared to the sets of  $\delta$  shown in Table 2.

Having selected the Euler angles for each mirror in case B and the sets of  $\delta$  and  $\epsilon$  that should produce the same total error in Case A as in Case B, we can make the comparison. Since the axes of the adjusting screws necessarily point in different directions in the laboratory for Case A and Case B, we expect to find different x, y and z errors when we compare Table 4 to Table 2. However, we expect the total error, i.e., the quadrature of the two errors, in Case A to be the same as the quadrature of the errors for Case B. Tables 3 and 4 give the results for Case B in the same fashion as do Tables 1 and 2 for Case A.

The Euler angles ( $\alpha$ ,  $\beta$ ,  $\gamma$ ) corresponding to Table 3 are, in degrees, (75.36119, 81.57894, 30.36119) and (151.3250, 148.6003, 73.67513) for the first two mirrors, respectively. The Euler angles for the third mirror are identical to those for the first mirror. Note that the errors in Table 4 are very different from Table 2, but in each row the sums of their squares agree between Tables 2 and 4 within roundoff errors.

Some numbers in Table 3 will help to elucidate the discussion above. The normals in Case A after transformation with an Euler matrix having  $45^\circ$  for each of  $\alpha$ ,  $\beta$  and  $\gamma$  will be (0.2500000, 0.9571068, 0.1464466), (0.4571069, -0.2500000, 0.8535534) and (-0.2500000, -0.9571069, -0.1464466) for the three mirrors, respectively. Note that the bottom row in Table 3 for mirror 1 matches the first of these normals, but the signs are opposite for mirrors 2 and

Table 4: Errors for Case B. Note the signs of  $\delta$  here compared to Table 2, as discussed.

<i>mirror</i>	$\delta$	$\epsilon$	<i>err<sub>x</sub></i>	<i>err<sub>y</sub></i>	<i>err<sub>z</sub></i>
1	0.0	1.0	0.7502	2.7052	0.4115
2	0.0	1.0	-1.2950	0.7051	-2.4171
3	0.0	1.0	-2.2947	-0.2969	-3.8302
1	1.0	0.0	-1.2064	0.2067	0.7083
2	-1.0	0.0	-3.6222	0.6172	2.1208
3	-1.0	0.0	-7.2436	1.2289	4.2466
1	1.0	1.0	-0.4977	2.9111	1.1176
2	-1.0	1.0	-4.9232	1.3233	-0.2927
3	-1.0	1.0	-9.5431	0.9334	0.4171

3. On the other hand, the second rows for all three mirrors are the same, meaning that the Ysides are all the same. Consequently, the Xsides have to be the same for mirror 1 but opposite for mirrors 2 and 3, compared to a 45°, 45°, 45° rotation of Case A. For this reason, the signs of  $\delta$  in Table 4 were chosen as shown. Again the approximate additivity in errors is seen in Table 4 as in Table 2. The check on the middle rows in Table 3 is that the 45°, 45°, 45° Euler matrix operating on (0,1, 0), the Yside in the REFERENCE position, is (-0.8535534, 0.1464466, 0.5000000). As discussed, only the 0.5000000, along with the desired bottom row of Table 3, were used as the four inputs into the process of finding the Euler angles to form Table 3. It is gratifying that the other elements of the middle rows in Table 3 match the Yside vector just mentioned.

The process that lead to Tables 3 and 4 illustrates some characteristics of the Euler matrix. Alternatively, we could have obtained the desired results by the following change of Euler angles. Retain the first mirror's Euler angles that lead to Table 3. For the Euler angles of the next two mirrors, add 180° to  $\beta$ . Consideration of the second of the three rotations that define the Euler set of three rotations will show that this will reverse the direction of the normal to these two mirrors. But this will result in the third rotation through  $\gamma$  being reversed in direction, so we compensate by changing the sign of  $\gamma$  for the last two mirrors. If then the signs of  $\delta$  in Table 4 are made the same as in Table 2 and the program is rerun, all of the 27 errors in Table 4 will be just the same as the errors in Table 2 within roundoff. And the signs of the matrix elements in the top rows and in the bottom rows of mirrors 2 and 3 in Table 3 will be reversed, as they should be.

## 8 REALISTIC FTPC CASE

Next we calculate a realistic case formed from a hypothetical but reasonable design of the laser system for the Forward TPCs (FTPCs). One objective is to get an accurate idea of how much deviation of the laser beam will result from various combinations of errors, for whatever reason, in the alignment of each mirror compared to the TUNED situation where all the mirrors are correctly positioned and oriented. The same program is used for this case as was used for the test cases above. It is possible that this program could be used as a basis for remote control of the orientations of some of the mirrors if the system wanders from the TUNED orientations and locations during continued operation. Such remote control will not be pursued further here.

Figure 1 shows this possible design in schematic form. Only enough detail will be given to show how the ideas discussed fit into a realistic case. The xy, yz and xz projections are shown to aid in visualization. The laser lies near the STAR floor and is at the initial point L of the entire path in Fig. 1. Paths 12 and 23 are mounted to the outside face of the pole tip of the STAR magnet solenoid. Path 34 is parallel to the RHIC beam (positive z direction), and mirror 4 is close to and mounted to the outside face of the FTPC. Path 45 takes the beam parallel to this face to a pair of mirrors, 5 and 6, which take the beam to the opposite side of the circular flange of the front face (circle in Fig. 1) , and direct the beam radially inwards inside the FTPC and in the xy plane along path 67.

The entry point of the beam into the FTPC is slightly downstream of mirror 6. The laser beam is  $\approx 20$  mm diameter upstream of mirror 4 and is collimated to 7 mm diameter at the entry point. In path 67 there are five 1-mm diameter mirrors at five different radii inside the FTPC<sup>[3]</sup> to pick off five portions of the 7-mm beam to produce five thin beams at various radii in nearly one plane (containing the RHIC beam). The one of these five beams nearest the RHIC beam is represented by the 1100-mm path departing from mirror 7 and traveling through the FTPC in the positive z direction. This beam 7E is 1 mm in diameter (minor diameter of the ellipse of mirror 7) and it provides a straight, calibrating track of ionization in the FTPC. The other beams <sup>[3]</sup> are not shown nor considered here although this same program has no problem in dealing with them.

This design is schematic, but it is realistic enough for the purpose of illustrating the propagation of the laser



Figure 1: (a), (b) and (c) are the  $xy$ ,  $xz$  and  $yz$  projections, respectively, of a portion of the hypothetical system. The path lengths are given in Table 5. The magnitudes of the angles between a path and the horizontal ( $xz$  plane) are  $30^\circ$  for 12, and  $15^\circ$  for 45 and 67. All lines drawn in Fig. 1 that appear to be parallel to one of the  $x$ ,  $y$  or  $z$  axes are indeed so. The dashed 4C is a monitoring beam leading to a CCD camera at C. Beam 4C is in the  $xy$  plane. (d) These seven unit vectors are the directions of the Ysides of the mirror mounts, designated by their labels in panels (a), (b) and (c) of this Figure. All seven vectors are in the  $xy$  plane, arbitrarily. Measuring clockwise from the positive axis, they are  $120^\circ$ ,  $240^\circ$ ,  $180^\circ$ ,  $255^\circ$ ,  $75^\circ$ ,  $105^\circ$  and  $105^\circ$ , reading from mounts 1 to 7.

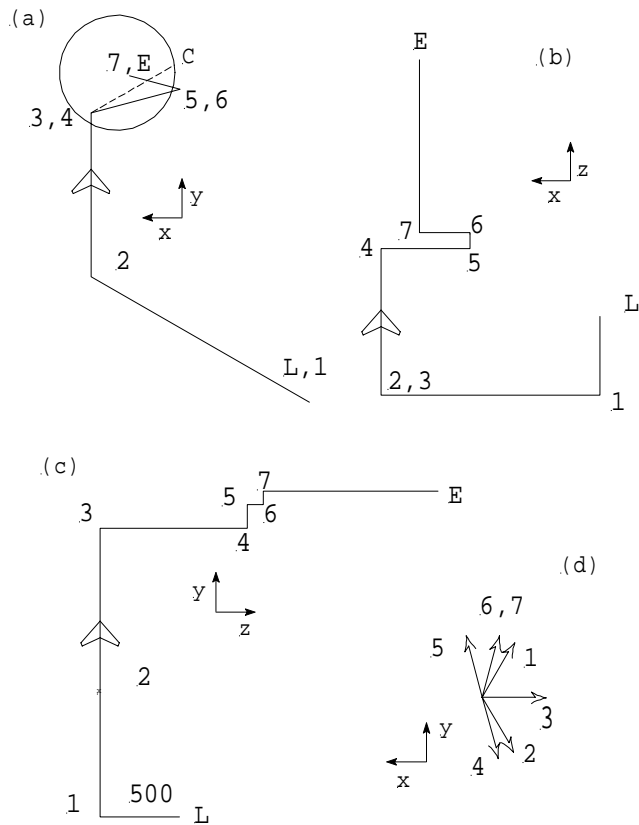


Table 5: Euler angles (degrees) for each mirror in the real FTPC example. D = distance (mm) to reach this mirror. The distance traveled after mirror 7 is 1100 mm from 7 to E.

<i>Mirror</i>	$\alpha$	$\beta$	$\gamma$	<i>D</i>
1	30	45	0	500
2	150	90	0	1590
3	90	135	0	1040
4	165	135	0	930
5	-15	45	0	580
6	15	-45	0	100
7	15	-45	0	330

Table 6: Euler matrix elements for the real FTPC example. The seven digits carried are rounded to three here, although seven are needed for accurate calculation.

<i>Mirror1</i>			<i>Mirror2</i>			<i>Mirror3</i>		
0.612	0.354	-0.707	0.000	0.000	-1.000	0.000	-0.707	-0.707
-0.500	0.866	0.000	-0.500	-0.866	0.000	-1.000	0.000	0.000
0.612	0.354	0.707	-0.866	0.500	0.000	0.000	0.707	-0.707
<i>Mirror4</i>			<i>Mirror5</i>			<i>Mirrors6and7</i>		
0.683	-0.183	-0.707	0.683	-0.183	-0.707	0.683	0.183	0.707
-0.259	-0.966	0.000	0.259	0.966	0.000	-0.259	0.966	0.000
-0.683	0.183	-0.707	0.683	-0.183	0.707	-0.683	-0.183	0.707

beam through a system of seven mirrors in a three-dimensional array, as well as the effects of tilting any mirror or combination of mirrors slightly about either or both of each mirror's two adjustment axes. A more detailed representation would show three beams in the xy plane, not one, emanating from three close spaced mirrors near position 4 of Fig. 1. These beams would be roughly 120° apart in order to produce three radial planes in the FTPC with five beams in each each plane instead of the single radial plane of five beams mentioned above. Thus, Fig. 1 shows one beam, 7E, selected from the fifteen beams just discussed. A further simplification to make the system and the matrix elements and direction cosines easier to visualize is to have each beam drawn in Fig. 1 lie in a plane parallel to some two of the three coordinate axes drawn in Fig. 1. There would also be a fourth mirror (not shown) near position 4 with a fourth beam going across the outside of the circular face of the FTPC to a monitoring CCD camera C on the periphery of the circular face. This beam is the dashed line 4C in the xy plane in Fig. 1.

One might wonder why it is useful to discuss precisions of a fraction of a millimeter for the locations of the broad beams between the laser and mirror 7. The reason is that a few-mm ball is placed in the center of the broad beam near the laser, and this produces a Poisson spot <sup>[1,4]</sup> of 0.2 mm diameter in the center of the broad beam. The Poisson spot is used to monitor the precise position of the beam by using miniature CCD cameras at various points (each near a mirror) in the system at least up to and including a distribution box near mirror 4. The major checker of the beam vector is at the two ends of path 4C.

The direction of the normal to each mirror determines how its incident beam is deflected, and this is determined by only Euler angles  $\alpha$  and  $\beta$ , as discussed above. Euler angle  $\gamma$  determines the orientation of the two axes, Xside and Yside, about which its mirror can be rotated by twisting each or both of the two adjustment screws. Arbitrarily, but without loss of generality,  $\gamma$  is chosen here to be zero for each mirror. This means that the Yside of the mirror mount is in the xy plane always. This again makes for ease of visualization, but any  $\gamma$  is satisfactory for operation of this computer program. In a real system,  $\gamma$  would often not be zero. The Euler angles for each mirror are given in Table 5.

The distances of flight between points in the system in the TUNED positions are also given in Table 5. The projections of these distances are shown in Fig. 1. For simplicity, the beam is deflected through 90° at each mirror except mirror 2, where it is deflected through 60°. Of course, this is not a requirement of the method of analysis, but is used for easy visualization. This configuration is close enough to a possible real system to illustrate the aspects of a real system.

The Euler matrix elements for each of the mirrors are given in Table 6. Note that each pair of rows for a mirror are orthonormal, as is each pair of columns. This is checked by the program to one part per million for consistency. Recall that the first row for each mirror is also the direction cosines of the Xside, the second row is the direction cosines of the Yside, and the third row is the direction cosines of the normal to the mirror, all being in the TUNED configuration.

Table 7: Direction cosines of each beam after reflection from its mirror.

<i>Mirror</i>	<i>Directioncosines</i>		
1	0.866	0.500	0.000
2	0.000	1.000	0.000
3	0.000	0.000	1.000
4	-0.966	0.259	0.000
5	0.000	0.000	1.000
6	0.966	0.259	0.000
7	0.000	0.000	1.000

Table 8: The adjustment angle (mrad) about the Xside is adjX ; the adjustment angle about the Yside is adjY. The differences between the position of striking the mirror n+1 with and without the adjustment of mirror n are  $err_x$ ,  $err_y$  and  $err_z$  (mm). These three errors in quadrature give the total error,  $err_{tot}$ .

<i>Mirror</i>	<i>adjX</i>	<i>adjY</i>	$err_x$	$err_y$	$err_z$	$err_{tot}$
1	1	0	-2.243	-3.885	-0.016	4.486
2	1	0	2.080	0.000	0.000	2.080
3	1	0	-1.317	0.001	1.272	1.831
4	1	0	0.212	0.793	0.001	0.820
5	1	0	-0.037	-0.136	-0.071	0.158
6	1	0	-0.120	0.451	0.001	0.467
7	1	0	0.404	-1.502	-0.001	1.555
1	0	1	0.000	0.000	-3.180	3.180
2	0	1	0.001	-1.039	-1.039	1.469
3	0	1	0.001	1.861	0.482	1.922
4	0	1	1.118	-0.299	-1.158	1.637
5	0	1	0.194	-0.052	0.174	0.265
6	0	1	-0.636	-0.170	-0.659	0.931
7	0	1	2.125	0.570	-0.002	2.200

The direction cosines of each beam after reflection from its mirror in the TUNED configuration are in Table 7. They will be seen to match the layout of Fig. 1(a-c). The beam incident on mirror 1 has direction cosines (0.000, 0.000, -1.000). Note that this set and the seven sets in Table 7 are normalized to unity, as required. This is checked by the program to one part per million for consistency.

Next we try adjusting some of the 14 screws for these 7 mirrors and let the program calculate the differences between the coordinates of the point where the beam (Poisson spot or beam center) strikes the mirror in the TUNED position given by Table 5, and also represented by Tables 6 and 7. In each of the following examples, the adjustment is by an angle of 1.000 milliradian, with a positive sign denoting that the bottom rule for the screw rotation is parallel to the direction cosine of the appropriate Xside or Yside of its mirror. The first test is to check the direction and amount of error produced by adjustment of each mirror. That is, Table 8 shows the error in position of actually striking mirror n+1 as the result of an adjustment of mirror n when the beam incident on mirror n is a TUNED beam. The mirror index in Table 8 is n. For mirror 7 the errors are measured after drifting 1100 mm to point E in Fig. 1. Conditions in Table 8 are simple enough that one can also check the results for sign and size by using a hand calculator.

Figure. 1(d) shows the direction of each Yside, obtained from Table 6. Recall that each Yside is in the xy plane. The direction of the Yside vector is the direction of a positive rotation around Yside producing adjY in Table 8.

Table 9 shows the results of giving every mirror the same adjustment. In contrast with Table 8 showing the error resulting from adjusting a single mirror and measuring at the next mirror, Table 9 follows the beam all the way through the system, listing the accumulated error due to every mirror having a 1.000 milliradian adjustment. The accumulated error in the position of the beam after it has traversed the FTFC is seen to be 5.045 mm when every mirror is adjusted by 1 mrad about its Xside axis, but 13.080 mm when instead every mirror is adjusted by 1 mrad about its Yside. Stated another way, if somehow each mirror got bumped out of its TUNED condition by a twist of 1 mrad about its Yside, the resulting displacement of the laser beam after traversing the FTFC would be 13.080 mm.

Next we adjust every mirror by +1 mrad about its Xside and by +1 mrad about its Yside. The results are in the top half of Table 10. Note that each  $err_x$  in this is roughly the sum of the values of  $err_x$  on the top half and

Table 9: Cumulative errors as the beam goes through the system. The top half has adjustment only in the adjX column. The bottom half has adjustment only in the adjY column. In a given row is the mirror index and its adjX and adjY, followed by the four accumulated errors in position measured at the succeeding mirror. In the case of mirror 7, the errors are measured at point E after traversing the FTPC.

<i>Mirror</i>	<i>adjX</i>	<i>adjY</i>	<i>err<sub>x</sub></i>	<i>err<sub>y</sub></i>	<i>err<sub>z</sub></i>	<i>err<sub>tot</sub></i>
1	1	0	-2.251	-3.890	-0.002	4.494
2	1	0	-1.639	0.000	-0.003	1.639
3	1	0	-2.411	0.000	2.328	3.352
4	1	0	-2.679	0.791	2.793	3.950
5	1	0	-2.758	0.791	-2.457	3.777
6	1	0	-3.152	1.241	-2.720	4.345
7	1	0	-4.063	1.241	-2.721	5.045
1	0	1	0.006	0.003	-3.180	3.180
2	0	1	0.010	-6.294	-6.281	8.891
3	0	1	0.014	-7.228	-1.881	7.469
4	0	1	1.125	-8.103	-3.191	8.781
5	0	1	1.522	-8.312	-0.680	8.477
6	0	1	2.162	-9.155	-0.280	9.411
7	0	1	6.417	-11.394	-0.291	13.080

on the bottom half of Table 9, although they do differ beyond their uncertainties. The same applies to  $err_y$  and to  $err_z$ . So again the errors are approximately additive. It is likely that this is an accident of the arbitrary choice of the directions of the Ysides, but runs to examine this have not been made.

It is of some interest to see how large the errors might be in the laser beam position after traversing the FTPC, while keeping only 1 mrad for each adjustment but varying the signs. This is not worth exhaustive study, but we can approximate this by using Table 8. That is, for the bottom half of Table the adjX signs were chosen to be the same as the  $err_x$  signs on the top half of Table 8. Similarly the adjY signs were chosen the same as the  $err_y$  signs on the bottom half of Table 8. The justification for this choice is not compelling, and the choice was made only as a first try to keep both  $err_x$  and  $err_y$  increasing as the beam moves through the system. Recall that there is nothing systematic in the relation of the direction of the Xside or the Yside to the laboratory coordinate frame, so correlating the mount-fixed Xside and Yside to the laboratory-fixed  $err_x$ ,  $err_y$  and  $err_z$  is a debatable criterion for maximizing the errors. Nevertheless, the results given on the bottom half of Table 10 show rather large errors, culminating in 38 mm total error at the end.

## 9 STABILIZING EFFECT OF 1-mm MIRROR

The last row in the bottom half of Table 10 shows the x, y, z and total errors in the coordinates of the center of the beam if mirror 7 were of large diameter and if there were no collimator. However, mirror 7 is only 1 mm in diameter. So the question becomes where would this same set of adjX adjY put the beam that actually is reflected by this small mirror 7? That is, we retain the same direction cosines of the beam impinging on mirror 7 as in the bottom half of Table 10, but force the reflection to occur at the center of mirror 7. This is the actual situation because mirror 7 is so small in diameter. The resulting deflection of this 1-mm beam after traversing the FTPC is -8.66 mm in the radial direction and 5.76 mm in the azimuthal direction, these being the departures from the beam location after the FTPC in the TUNED situation.

Fig.1 shows that the radial path 67 is only 15° away from the x direction, so these deflections are to be compared approximately to -20.6 and 26.4 mm in Table 10. (Note that the positive x direction is nearly the negative radial direction here). In other words, the smallness of mirror 7 provides a reduction in the calibration error by a factor of 2.4 in the radial direction and 4.6 in the azimuthal direction. For the top half of Table 9, the factors are 4.6 and 5.3, respectively. For the bottom half of Table 9, the factors are 1.8 and 3.5. For the top half of Table 10, the factors are 0.88 and 3.4. Thus, the smallness of mirror 7 usually reduces the error in calibration of the FTPC, and often by a significant amount. However, for this last case of a factor 0.88, the beam leaving a large version of mirror 7 would be, radially speaking, off center and with the wrong slope but such as to nearly compensate each other at the far end of the FTPC.

Table 10: Effects of having all 1 mrad misalignments of mirrors. (a) All same sign: on the top half, all 14 twist angles, adjX and adjY, of misadjustment of the screws have the same sign. (b) Signs to give large errors: on the bottom half the adjX and adjY signs are chosen to make the  $err_x$  and  $err_y$  increase in magnitude at each succeeding mirror.

Mirror	adjX	adjY	$err_x$	$err_y$	$err_z$	$err_{tot}$
1	1	1	-2.243	-3.883	-3.174	5.494
2	1	1	-1.629	-6.299	-6.288	9.048
3	1	1	-2.403	-7.237	0.436	7.637
4	1	1	-1.549	-7.325	-0.411	7.498
5	1	1	-1.254	-7.523	-3.162	8.256
6	1	1	-1.009	-7.917	-3.029	8.537
7	1	1	2.332	-10.160	-3.036	10.858
1	-1	-1	2.270	3.916	3.186	5.535
2	1	-1	5.835	6.329	6.308	10.672
3	-1	1	10.261	10.913	-7.083	16.569
4	1	-1	12.133	14.907	-7.870	20.770
5	-1	-1	12.341	15.995	16.075	25.818
6	-1	-1	13.686	18.637	18.028	29.319
7	1	1	20.562	26.437	17.979	38.012

## 10 ABILITY TO STEER ERRANT BEAM BACK TO TUNED POSITION BY ADJUSTMENT OF TWO MIRRORS

If mechanical mounts in the mirror system should somehow shift, we want the capability to compensate by adjX and/or adjY in some mirrors such that the beam in the FTPC at station E is returned to its proper position. Such compensation must be remotely controlled due to limited access to the FTPCs during RHIC operation. Also the compensation should be made as far downstream in the system as possible, consistent with the constraint of available space for such mechanical control. The reason is to position the control downstream of as many mechanical perturbations as possible.

In many systems, it is necessary to control the five variables of a beam vector, viz., (x, y, z) and its two polar angles. Here (x, y, z) is the location where the beam center strikes some arbitrary, hypothetical plane, fixed in space. Such control requires (remote) adjustment of adjX and adjY of at least two mirrors – the first mirror is to restore the center of the errant beam to the center of the second mirror, and the second mirror is to restore the proper direction of the beam reflecting from this mirror. In this statement, it is assumed that whenever the proper adjX and adjY are provided to the second mirror, the beam incident on this mirror always strikes it at its center. Such is the property of a gimbal mount. Thus, the five control variables are adjX and adjY for two mirrors (four, in all) plus the distance from the point where the beam strikes an arbitrary, fixed plane to the point where the beam strikes the second mirror. This matches the five degrees of freedom of the beam vector leaving the second control mirror.

However, in the preceeding section we saw that for the present system the primary need is to obtain the correct direction of the beam in path 67. One implication of this is that we do not have to adjust accurately the distance to the second controlling mirror, so the four variables adjX and adjY of the two controlling mirrors are sufficient. With these four adjustments set properly, the distance parameter does not affect the direction of the beam leaving the second control mirror, it only affects the centering of the reflected beam. We assume here that there is no shift of any of the mirrors downstream of the two remotely controlled mirrors.

The ideal mounting of the two remotely controlled mirrors would be to the rigid face of the FTPC. This would minimize the probability of shifting of mirrors downstream of the two control mirrors. However, there is limited space near the circular face of the FTPCs, so we will consider in this analysis that mirrors 2 and 3 are the ones to be remotely controlled. Consider that mirror 1 has somehow shifted its orientation by only 1.4 mradian. Specifically consider that adjX=-1 and adjY=-1 through some accident, but all other mirrors remain in their TUNED configuration. This could represent a more general shift somewhere in the system upstream of mirror 2. The result after the beam traverses the FTPC is:  $err_x=8.0$ ,  $err_y=11.4$ ,  $err_z=8.6$ ,  $err_{tot}=16.4$ , radial calibration error=-2.1 and azimuthal calibration error=1.7, all in mm. The correction for this accident is: mirror 2 is given adjX=-1.7790, adjY=5.0700; mirror 3 is given adjX=-1.5090, adjY=1.5377. The result is that all six of the above errors become -0.001, -0.002, -0.001, 0.003, 0.0006 and -0.001 mm. In other words, this accident has been remedied to better than 3 microns by this remote adjustment of mirrors 2 and 3. The ability to remedy such an accident does not depend on the direction

of the accidental deflection from TUNED produced at mirror 1. It would work equally well for any combination of adjX and adjY at mirror 1. As part of this correction system, there would be CCD cameras looking at the Poisson spot very near to each of mirrors 3 and 4 to confirm the centering of the beam at these two mirrors.

As a second check, CCD camera C of Fig. 1(a) would be employed. An additional mirror (not shown) would be near mirror 4 to produce the dashed beam 4C for this check. The path length 4C of this monitoring beam is 606 mm. This establishes a reference vector confirming that the beam onto mirror 4 has the correct properties. The precision of this check is about  $\sqrt{2} \cdot 0.2 / 606 / 5 = 0.1 \text{ mrad}$  because camera C could determine the center of the Poisson spot to about 1/5 of its diameter, as could the camera near 4.

## 11 EFFECT OF POSSIBLE SHIFTING OF POLE PIECE

The mounts for mirrors 2 and 3 are located on the magnet pole piece. Perhaps once or twice per year this pole piece will be removed and later put back onto position. So the question is how much this will perturb the laser distribution system. A pole is held in place with four heavy pads located symmetrically around its circular periphery. These are designed <sup>[5]</sup> for a maximum deflection of 0.005 inch each, due to axial forces on the pole tip. The normal to the pole face could then change its direction by  $\leq 0.005 / 100 = 0.05 \text{ mrad}$  due to magnetic forces. They are likely to deflect by similar amounts, giving even less change in tilt than this. The change in axial station of the pole tip due to removal and relocation is about 0.001 in. The x and y coordinates of any given point of the pole are affected by the clearance between the bolts at these four pads and their bolt holes. This may be a few mm. However, the surveyors can locate a point to within 0.005 inch with reasonable angles of sight. So whenever the infrequent pole piece location is cycled, each of the two boxes containing mirrors 2 or 3 can be surveyed, and if necessary put back to their original (x, y, z) coordinates within 0.005 inch (0.13 mm), which is less than the diameter of the Poisson spot. These are very small errors which can easily be remedied by readjustment of the already remotely controlled angles of mirrors 2 and 3.

To see that this is possible, assume that the system composed of the FTFC and mirrors 7, 6, 5 and 4 is rigid against replacement of the pole piece. And consider hypothetically shining the laser beam into mirror 7 from point E on the opposite end of the FTFC, with the beam inside the FTFC being exactly the same vector (rotated end for end through  $180^\circ$ ) as during the real TUNED operation of the laser system. Then the question becomes whether manipulation of some combination of the four angles adjX and adjY of mirrors 3 and 2 could result in a backwards-beam vector leaving mirror 1 towards L which is exactly the same as the input laser beam vector L1 in actual operation (after this latter beam is rotated end for end by  $180^\circ$ ). From consideration of the above analysis of steering, the answer is clearly yes. This requirement is easily met. Mirror 1 is also available but its readjustment should not be needed.

The other question is whether there is enough monitoring described so far to assure that this realignment is accomplished. The requirement is to determine that the vector leaving mirror 4 in real operation has the same five coordinates (but emphasizing the direction more than (x, y, z)) after the replacement of the pole piece as it had before. This information is provided by the CCD camera monitoring the Poisson spot near mirror 4 and the camera C. If mirror 3 should shift, the only requirement for being able to compensate by only adjusting mirrors 2 and 3 is that mirror 3 should not have changed its x,y coordinates by an appreciable fraction of the 20-mm diameter of the laser beam there. That is, if mirror 3 had moved a small distance **G**, the Poisson spot at this mirror should be steered to a point **-G** away from the original center of this mirror. This would restore the vector measured at sites 4 and C.

In conclusion, the possible shift of the pole piece does not appear to be a difficult problem.

Again it is emphasized that these considerations are of a possible design which will likely differ from the final design of the FTFCs laser calibration. However, it is sufficiently near any possible final design that the performance numbers here are expected to be closely representative of the final design.

## REFERENCES

1. A. Lebedev, private communication. Nuclear Science Symposium, IEEE 1996, p.499-506, vol. 1.
2. MATHEMATICAL METHODS OF PHYSICS, J. Mathews and R.L.Walker, W.A. Benjamin, Inc., New York, 1970
3. Forward Time Projection Chamber for the STAR Detector, Proposal to STAR by the STAR FTPC Collaboration, January, 1998, MPI-PHE/98-3
4. A.E. Siegman, LASERS, Mill Valley, Calif.: University Science Books, 1986
5. Ralph Brown, STAR Chief Mechanical Engineer, private communication.